Bulletin Géodésique (1993) 67:31–40

Bulletin Géodésique

The method of free-positioned point masses – geoid studies on the Gulf of Bothnia

Rüdiger Lehmann

Geo-Forschungs-Zentrum Potsdam, Telegrafenberg A17, O-1561 Potsdam, FRG

Received June 18, 1992; Accepted December 2, 1992

Abstract

Gravity data inversion methods using spatial source distributions are frequently investigated and applied in Geodesy. Nearly all of them construct a fixed geometry for the sources. It was shown that this is not at all necessary. We give an approach to the problem of geoid determination based on free-positioned point masses. The algorithm available is extended and refined in order to make it applicable to more ill-designed and complex problems than addressed so far. We introduce concepts to handle different data accuracies, non-uniform data coverages, and different data types. The Gulf of Bothnia serves as an area of investigation. We determine a pure gravimetric geoid solution as well as a combined solution based on gravimetric and altimetric data. The problem of gross error detection in the altimetry is treated. The prediction accuracies obtained prove the method to be suitable for such a problem. *

1 INTRODUCTION

1.1 Some earlier Baltic geoid computations

Many arguments speak in favour of the Baltic Sea as an "open air laboratory" (Vermeer 1983) for methods of geoid determination. It is both geographically suited (e.g. small tidal motion) and fairly well covered with all kinds of data (gravity, altimetry, tide gauge data etc.). A considerable amount of work has already been done towards a Baltic Sea geoid. Anderson and Scherneck (1981) provided a SEASAT-geoid. Vermeer (1983) compared his altimetric geoid with an earlier computed gravimetric geoid for Finland (Vermeer 1982). (For more details see also Vermeer 1984). Elsewhere the problem is addressed in a larger scale (Tscherning 1985, Forsberg 1990). For this investigation we restrict ourselves to the geoid of the Gulf of Bothnia. An extension to the whole Baltic Sea area is in preparation.

*extended version of a paper presented at the 1st Continental Workshop on the Geoid in Europe, Prague 11–14 May 1992.

1.2 Why taking free-positioned point masses ?

The geodesists using observations related to the gravity field of the Earth in order to predict unobserved gravity field related quantities are solving an *inverse problem* (in the very sense of the term, i.e. the problem of inferring values for unobserved quantities from observed values, see e.g. Tarantola 1987). Inevitably, they have to put up with a finite or even a quite small number of such observations. Therefore it is necessary to assume something about the field, usually something that minimizes the numerical effort or allows to apply a mathematical relationship. For example, the gravitational field of the Earth is treated as being

smooth (in the sense of having a limited spectral bandwidth), or

a stationary process, or

a sum of a finite number of base functions (e.g. spherical harmonics).

Certainly, none of them is true. The field is just assumed to be *simple* in some sense. If one wants to incorporate geophysical information concerning the density distribution of the Earth, it seems to be preferable not to claim simplicity for the *gravity field*, but for its *sources*. This implies an assumption like:

> The density distribution of the Earth is considered simple, if it consists of a small number of disturbing bodies of a simple shape.

We believe that point masses can advantageously be used as such bodies. Consequently, we will try to find a solution for the inverse problem, that is as simple as possible in the sense defined above: a gravitational field generated by the *smallest* possible number of point masses. Closely examined, the solution remains nonunique.

However, this is of no practical significance in larger scale problems, because the *simplest* solution can not be found anyway with a reasonable numerical effort.

The fundamental observation equations are nonlinear. Accordingly, we have to solve a *nonlinear* inverse problem.

1.3 A brief description of the algorithm available so far

The basic algorithm for free-positioned point masses was proposed by Barthelmes (1986). Here we can only outline it: The set of model parameters for N point masses with magnitude μ^i and positions $(x^i, y^i, z^i)^T$ can be expressed as $\mathbf{m}^N = (\mu^1, x^1, y^1, z^1, \ldots, \mu^N, x^N, y^N, z^N)^T$. Prior information for $\mathbf{m}$ is not available. $\mathbf{d}_{obs}$ denotes a set of N_d gravity anomalies with error covariance $\mathbf{C}_d = \sigma_d^2\mathbf{I}$ ($\mathbf{I}$ is the identity matrix). The corresponding estimates are related to $\mathbf{m}$ through $\mathbf{d}_{est} = \mathbf{g}(\mathbf{m})$, where $\mathbf{g}$ is a vector valid operator. The best solution for $\mathbf{m}$ in the maximum likelihood sense (least squares) can be found iteratively using the following equation

$$\mathbf{m}_{n+1} = \mathbf{m}_n + (\mathbf{G}_n^T\mathbf{G}_n + \mathbf{R}_n)^{-1}\mathbf{G}_n^T(\mathbf{g}(\mathbf{m}_n) - \mathbf{d}_{obs}) \tag{1}$$

Here the design matrix $\mathbf{G}_n$ consists of the derivatives

$$G_n^{ij} = \left(\frac{\partial g^i}{\partial m^j}\right)_{\mathbf{m}_n}, \tag{2}$$

where $i = 1, 2, \ldots, N_d$ and $j = 1, 2, \ldots, 4N$, while $\mathbf{R}_n$ denotes a stabilizing diagonal matrix according to the well known trust region method.

The problem is overdetermined ($N_d > 4N$) and well posed, except for some critical cases. However, if the initial guess $\mathbf{m}_0$ is selected improperly it converges very slowly. The idea is to perform a stepwise model determination:

1st step: Start with one point mass only. Choose its initial position in a proper depth below $\max|\mathbf{d}_{obs}|$. Set $\mathbf{m}_0^1 = (0, x_0^1, y_0^1, z_0^1)^T$. Determine $\mathbf{m}_\infty^1$ through a least squares iteration.

...

N-th step: Search for $\max|\mathbf{d}_{obs} - \mathbf{g}(\mathbf{m}_\infty^{N-1})|$. Place the N-th point mass in a proper depth below this observation point. Set $\mathbf{m}_0' = (0, x_0^N, y_0^N, z_0^N)^T$. Determine $\mathbf{m}_\infty'$ through a least squares iteration. The initial guess is $\mathbf{m}_0^N = ({\mathbf{m}_\infty^{N-1}}^T, {\mathbf{m}_\infty'}^T)^T$. Now determine $\mathbf{m}_\infty^N$ through a least squares iteration.

There is a variety of time saving options in the algorithm, for example, we do not need to perform too many iteration steps unless the final number of point masses is reached.

2 EXTENSIONS AND REFINEMENTS OF THE METHOD

The program system for free point mass adjustment by F. Barthelmes is used for the subsequent computations. It was already applied in a few practical studies (Barthelmes and Dietrich 1990), but it required some work to make it applicable to more ill-designed and complex problems.

2.1 Different data accuracies

If the data $\mathbf{d}_{obs}$ have individual error figures, we can simply introduce the error covariance $\mathbf{C}_d$ into eq. (1). But then the original algorithm fails. The reason lies in the stepwise nature of the algorithm. At the very beginning, where we have only a few point masses, it is the insufficient model rather than the measurement inaccuracy that causes the uncertainties in the results. After adding more and more point masses the situation changes, and in the long run the model error should become very small. If we assume Gaussian distribution with zero expectation and covariance matrix $\mathbf{C}_T$ for this type of error, eq. (1) changes to

$$\begin{aligned}\mathbf{m}_{n+1} \;=\; & \mathbf{m}_n + (\mathbf{G}_n^T(\mathbf{C}_d + \mathbf{C}_T)^{-1}\mathbf{G}_n + \mathbf{R}_n)^{-1} \times \\ & \times\mathbf{G}_n^T(\mathbf{C}_d + \mathbf{C}_T)^{-1}(\mathbf{g}(\mathbf{m}_n) - \mathbf{d}_{obs}).\end{aligned} \tag{3}$$

The problem is now to find $\mathbf{C}_T$. As the results will show, even the simplest choice can sometimes work fine:

$$\mathbf{C}_T = \sigma_T^2\mathbf{I}. \tag{4}$$

By this we assume the same model error for any observation neglecting possible correlations. We can think of several methods for finding a reasonable σ_T. One of them is applied in this study, it benefits from the fact, that we do not need to know the absolute error scale σ_0 (error of unit weight) for the model determination, but we can find an estimate for it, e.g. [1]:

$$\sigma_0^2 = \frac{(\mathbf{g}(\mathbf{m}_\infty) - \mathbf{d}_{obs})^T(\mathbf{C}_d + \sigma_T^2\mathbf{I})^{-1}(\mathbf{g}(\mathbf{m}_\infty) - \mathbf{d}_{obs})}{N_d - 4N} \tag{5}$$

The denominator expresses the degrees of overdeterminancy in the problem.

Usually the absolute errors are more or less known (e.g. from repeated measurements). We blame the model error for the remaining disagreement between this estimate and our knowledge. The idea is to change σ_T until agreement is reached.

Furthermore, the initial point mass searched for in the next step is now given by

$$\max|(\mathbf{C}_d + \mathbf{C}_T)^{-1/2}(\mathbf{g}(\mathbf{m}_n) - \mathbf{d}_{obs})|. \tag{6}$$

[1] Problems with nonlinearity appear to be small in this case, at least if $N_d \gg 4N$ (Lehmann 1992).

2.2 Non-uniform data coverage

It is well known that modelling a finite set of gravity anomalies in a local area can only reveal a certain spectral part of the potential function wanted, the limits correspond to the sampling intervals and the size of the area. Therefore the short wavelength part is mainly due to the terrain model whereas the long wavelength part comes from the reference model. Now we have to take care of the spectral content of the model computed from the local gravity anomalies. It should not contain much short wavelength power, otherwise it produces nonsense in the data gaps, and it should not contain long wavelength information, otherwise it produces nonsense outside the data-covered area. In many modelling methods it is fairly easy to do so, particularly in the frequency domain methods.

But even with point masses one can produce some sort of a limited spectrum by excluding deep and shallow masses. The maximum depth depends on the distance to the margin and the minimum depth depends on the local data density. Therefore, an admissible region $\mathcal{B}$ for the point mass positions has to be defined. The algorithm changes into a nonlinear least squares procedure with nonlinear constraints. $\mathcal{B}$ is established as a set of m (perhaps overlapping) *blocks* $\mathcal{B}= \mathcal{B}_1 \cup \ldots \cup \mathcal{B}_m$ bounded by meridians, parallels and geocentric ellipsoids (in fact, any region $\mathcal{B}$ may be approximated by such a set). The depthlimits D^i_{max} and D^i_{min} for $\mathcal{B}_i$ can be chosen with respect to the distance to the margin and the mean or maximum data spacing above $\mathcal{B}_i$, respectively. This automatically bans point masses below data gaps and close to or beyond the margin, where $D^i_{max} < D^i_{min}$. All other blocks will be referred to as admissible in the following. Nevertheless, short waves may occur to some extent through occupation of the upper depthlimit with pairs of point masses very close to each other and opposite signs (dipoles). This will do harm only if their magnitudes are relatively large. To prevent this, for any block a maximum absolute magnitude may be specified.

The initial depth of any new point mass is now related to the depthlimits rather than uniform in the whole area. (6) should be modified to

$$\max_{d_i \text{above } \mathcal{B}} |(\mathbf{C}_d + \mathbf{C}_T)^{-1/2}(\mathbf{g}(\mathbf{m}_n) - \mathbf{d}_{obs})|. \qquad (7)$$

2.3 Different data types

The further incorporation of other kinds of measurement such as altimetry does not pose any insurmountable problems. However, eq. (4) is no longer valid. For m different data types it must be extended to

$$\mathbf{C}_T = \begin{pmatrix} \sigma^2_{T1}\mathbf{I} & \ldots & \mathbf{0} \\ \vdots & \ddots & \vdots \\ \mathbf{0} & \ldots & \sigma^2_{Tm}\mathbf{I} \end{pmatrix} \qquad (8)$$

So we have to compute posterior error figures for any of the data types in order to obtain reasonable model errors.

Eq. (4) is also violated in another sense: By adding more and more point masses the model errors σ_{Ti} will decrease substantially compared to the beginning. But if we restrict all point mass positions to a region $\mathcal{B}$, it will decrease much faster for observations located above $\mathcal{B}$ than for all the rest. Therefore, it appears to be necessary to treat both kinds of observation as different in the sense of eq. (8). Further subdivisions may lead to a sort of local model errors, but now the method tends to become theoretically highly dubious.

3 A REFERENCE MODEL CONSISTING OF FREE-POSITIONED POINT MASSES

3.1 The global gravity field model

The global spherical harmonics gravity field model OSU89B (see e.g. Rapp et al. 1991) was converted to point masses with optimized positions on the basis of synthetic gravity disturbance observations. Details have been presented by Barthelmes et al.(1991a). Here we only recall the basic structure, it follows an idea of Heikinnen (1981) [2]:

The global point mass model consists of

7 point masses fitting the normal field GRS80 (situated equidistantly and equatorial-symmetrically on the mean rotation axis of the Earth, mean deviation of the level surface from the GRS80-ellipsoid is $\pm$2.0 mm, the maximum is 2.7 mm)

+100 point masses fitting OSU89B up to degree and order 20 (designed for high orbiting satellites, the mean orbital fit of a 30-day-arc of LAGEOS computed with the orbital progam system POTSDAM-5 turned out to be $\pm$69 mm instead of $\pm$62 mm using OSU89B itself)

+1000 point masses fitting OSU89B up to degree and order 60 (designed for low orbiting satellites, the geoid deviation from OSU89B up to degree and order 60 is $\pm$0.30 m)

3.2 The regional gravity field model for Europe

The European model consists of further 1000 point masses fitting OSU89B in the region of

latitude: 30°...75° longitude: −20°...50°

As in the global case the model was determined by means of synthetic gravity disturbance observations, computed from OSU89B. Details have been presented by Barthelmes et al. (1991b). The mean geoid deviation from OSU89B in this area (internal model fit) evaluated by means of 1000 synthetic prediction points was shown to be $\pm$0.19 m.

[2] In his study Heikinnen used 5+1654+41646 point masses in fixed positions without overdeterminancy.

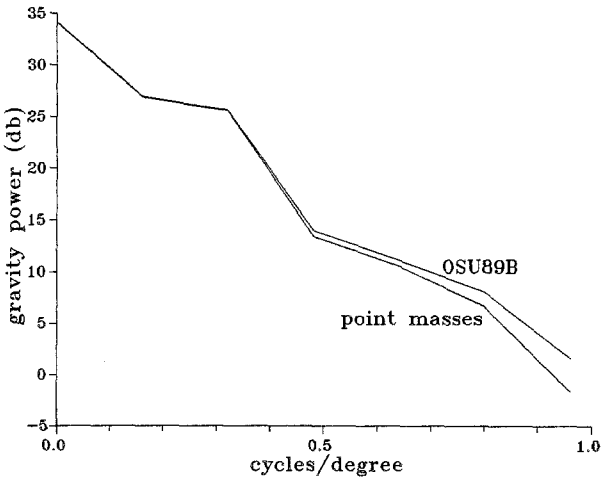

Figure 1: Power spectra of the spherical harmonics model OSU89B and the point mass reference model.

3.3 Evaluation of the reference model in the Baltic Sea area

First of all, we have to determine the accuracy of our reference point mass model (7+100+1000+1000 masses) in the Gulf of Bothnia with respect to OSU89B. A gravity grid is computed from both reference models in the area

latitude: 60°...66° longitude: 16°...26°

with a spacing of 0.25 degrees. The corresponding power spectral densities are shown in Fig. 1. Both are sufficiently similar. In fact, the corresponding geoid r.m.s. difference turns out to be ±0.15 m, this is substantially better than the real accuracy of the models (about ±0.35 m). It appears to be a challenge to update the whole reference model according to a newly available set of spherical harmonics. This was done at least for the magnitudes of the reference masses using OSU91A (Rapp et al. 1991), but (as one could more or less expect) a considerable improvement with respect to the Baltic Sea data was not achieved. The reason is quite obvious: The gain of information is not very important for this area. Therefore, such attempts have been abandoned.

4 A GRAVIMETRIC POINT MASS GEOID IN THE GULF OF BOTHNIA

4.1 The selection of gravity anomalies

In the Gulf of Bothnia we have a fairly non-uniform coverage of gravity anomalies. Nevertheless, it seems possible to compute a pure gravimetric geoid for comparison with altimetry data. For this purpose not only the gravity data in the sea area are to be taken into account, but also a margin in order to catch remaining long wavelength errors in the reference field. After an outlier test by means of collocation interpolation using a 3σ-criterion (the theory can be found in Tscherning 1990) we select 11245 gravity anomalies as shown in Table 1. In the following, zone 1+2, 3 and 4 will be referred to as the inner, medium and outer zones, respectively. The spatial data distribution is depicted in Fig. 2. Unfortunately, the mean spacing desired can not be achieved in certain regions. The local best standard deviations in land and sea area are in the range of ±0.1...±1.0 mgal and ±0.3...±2.5 mgal, respectively. In order to evaluate the interpolating properties of the computed point mass models we need some prediction values for comparison purposes. A set of prediction gravity stations is extracted from our observation set using the following criteria:

a mean spacing of about 50 km, and

a (quite stringent) rejection level of ±0.3 mgal on the formal observation errors stated.

This produced a set of 211 gravity prediction points. They represent the formal truth from now on, because their observation errors are supposed to be much smaller than the expected prediction inaccuracy. Their distribution (see Fig. 3) leaves a little bit to be desired, this is due to the overall poor observation accuracy in the northern part of the Gulf. Here we exclusively rely on the altimetry data as prediction quantities.

4.2 The reference field subtraction

In order to benefit from the possibility to represent both the global and the local gravity field by the same method, this is the described point mass technique in our case, the already mentioned point mass reference model for Europe is subtracted from the observations. Table 2 shows how the statistics of the observations change.

4.3 The terrain reduction

No doubt, it is highly recommendable to take into account density information, it can be treated as some kind of prior information for the model parameters. The best available information concerning the density is the shape of the physical surface of the Earth. It indicates where the density jumps from that of crustal rock (approx. 2.67 g/cm^3) to near-zero. Translated to prior information this means that point masses are not allowed to lie above this surface. Furthermore, we know something about the density for the topographic masses, constraining the magnitudes of the shallow point masses etc.

However, for these geoid computations it may lead too far. For the beginning it seems to be recommendable to rely on an already investigated and widely accepted method: the RTM-method (see Forsberg and Tscherning 1981, Forsberg 1984).

The procedure could be briefly outlined as follows:

Table 1: Selection of gravimetric observations in the Gulf of Bothnia region.

zone	distance to sea area	data selection	number of data
1	sea area itself	full set	3754
2	close to sea area (<50 km)	full set	2447
3	50 km...100 km	about 5 km mean spacing	2934
4	100 km...200 km	about 10 km mean spacing	2110

Table 2: Statistics of gravimetric observations.

	mean value (mgal)	std.dev. (mgal)	min. value (mgal)	max. value (mgal)
before reference field subtraction	-20.81	19.38	-83.2	81.0
after reference field subtraction	0.03	9.44	-39.5	67.3

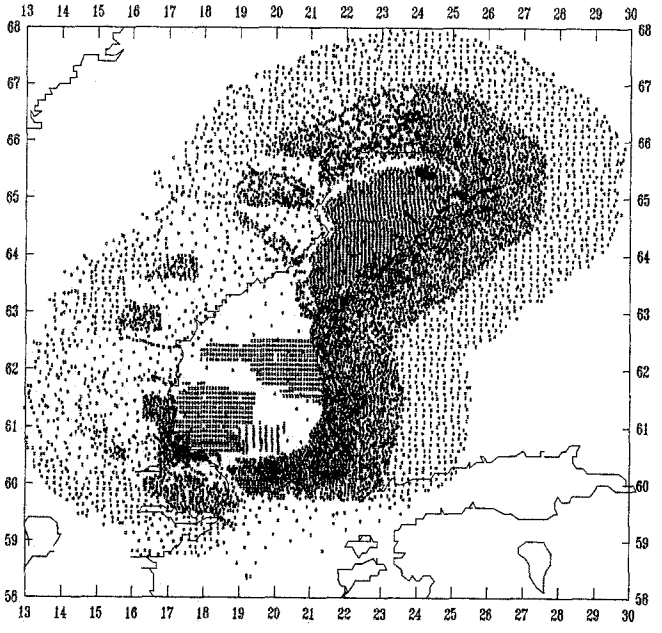

Figure 2: Spatial distribution of the gravimetric observations selected (11245 points).

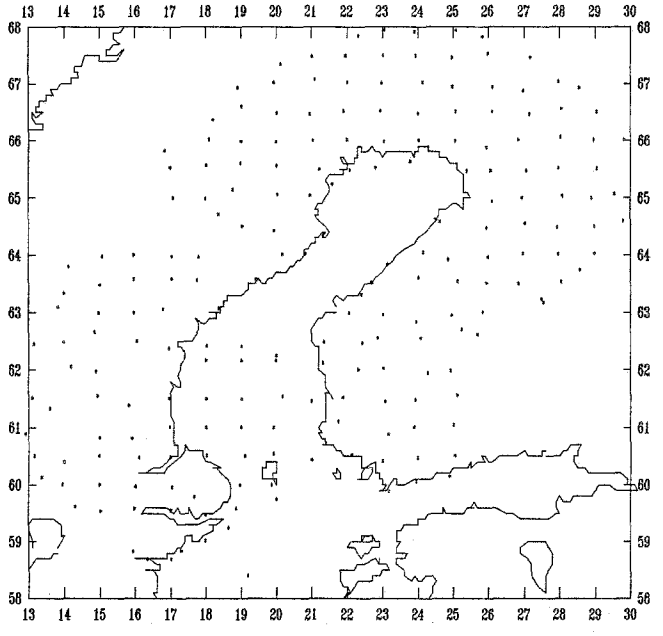

Figure 3: Spatial distribution of the gravimetric predictions selected (211 points).

Generate a smooth terrain grid on the basis of the "real" terrain grid. The smoothing operation is a simple moving average.

Interpolate the heights of the smooth terrain at the gravimeter sites.

Apply the terrain correction (remove mountains and fill up valleys).

Remove a simple Bouguer plate effect in order to obtain observations referring to the smooth terrain.

Restore the real terrain after prediction and change the predicted gravity values.

A detailed digital terrain grid (5 km×5 km) of the area under investigation is used. A constant density of 2.67 g/cm^3 is assumed and no bathymetric information is taken into account. The size of the moving average window is subject to investigation: If the smooth terrain is too smooth, a partial gravity effect is removed twice, both as rough terrain attraction and as reference field. If it is too rough, it will leave detailed field structures smaller than the gravity data spacing, which thus cannot be resolved. Therefore, we compute the statistics of the residuals after reduction with respect to differently smoothed terrains. As shown in Table 3 the best window size (least standard deviation and tolerable mean value) turns out to be (about) 110 km. Fig. 4 shows some corresponding power spectra.

Table 3: Residual gravimetric observations after RTM-reduction.

moving average window size (km)	mean value (mgal)	std.dev. (mgal)	min. value (mgal)	max. value (mgal)
50	0.61	8.70	-39.1	35.8
80	0.75	8.59	-38.3	35.7
110	0.94	8.53	-37.5	36.8
140	1.15	8.54	-36.7	37.3
170	1.41	8.61	-36.0	37.4

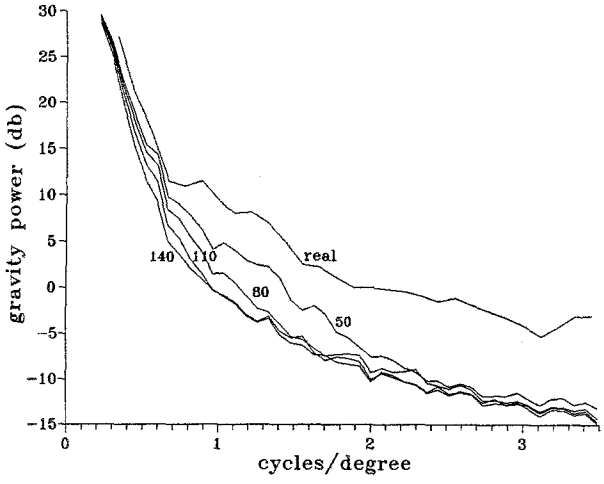

Figure 4: Power spectra of the real terrain and of certain smoothed terrains (curve label=moving average window size in km).

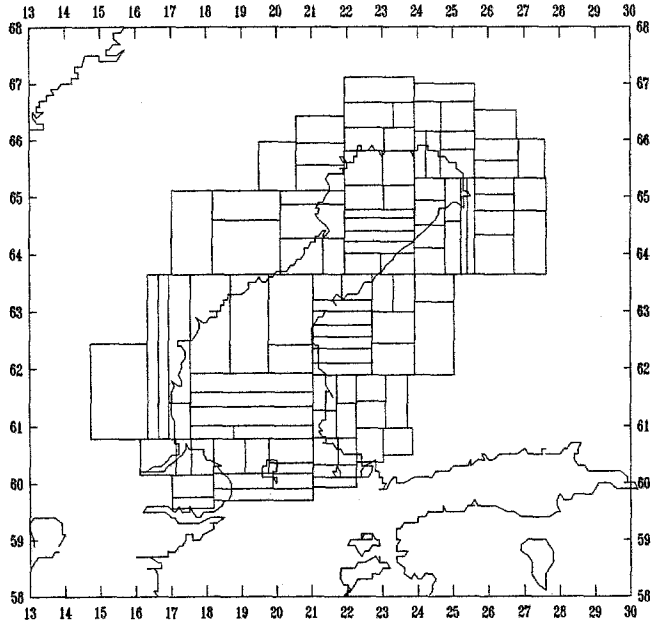

Figure 5: Subdivision in 103 blocks with about 90 gravimetric observations each. Only admissible blocks are drawn.

4.4 The determination of point mass limits and model errors

The area is divided into spherical rectangles. Starting with the smallest rectangle including all observations any rectangle is subdivided bisecting the number of observations as long as it exceeds 100. We choose the intersecting curve (parallel or meridian) maximizing the total volume of the resulting admissible region in order to give the model maximum "freedom". The result is shown in Fig. 5. The depthlimits are simply 1/5 of the distance to the margin and the mean data spacing, but at least half the maximum spacing. This leads to 8959 (about 80%) gravity anomalies above admissible blocks.

The model errors are determined separately for observations above and beside admissible blocks. This process is integrated in the iteration according to eq. (3), thus it practically consumes no extra computation time.

4.5 The SEASAT-altimetry data in the Baltic Sea

The data set consists of 2634 sea surface heights, each a mean of 10 radar measurements. They can to some extent be treated as geoid heights because the Baltic sea surface is little affected by ocean tides, currents, regional weather patterns, and the like (Anderson and Scherneck 1981). A standard crossover adjustment is performed, it rejects 11 observations. The error is supposed to be ±8 cm for any geoid height. Now, in the Gulf of Bothnia we have 920 adjusted data, their spatial distribution can be seen in Fig. 7.

First of all, we treat them as prediction quantities in order to evaluate the computed gravimetric geoid.

4.6 The results

It is interesting to see how several gravity prediction error figures behave during increasing the number of determined point masses. This is shown in Fig. 6a. For 1000 point masses we obtain ±2.3 mgal, ±3.9 mgal and ±7.7 mgal for the inner, medium and outer zone, respectively. The substantial change for the "worse" towards the margin is as expected, the reference field is more and more left unchanged. The estimated model error *above* the admissible blocks decreases rapidly. Not so *beside*

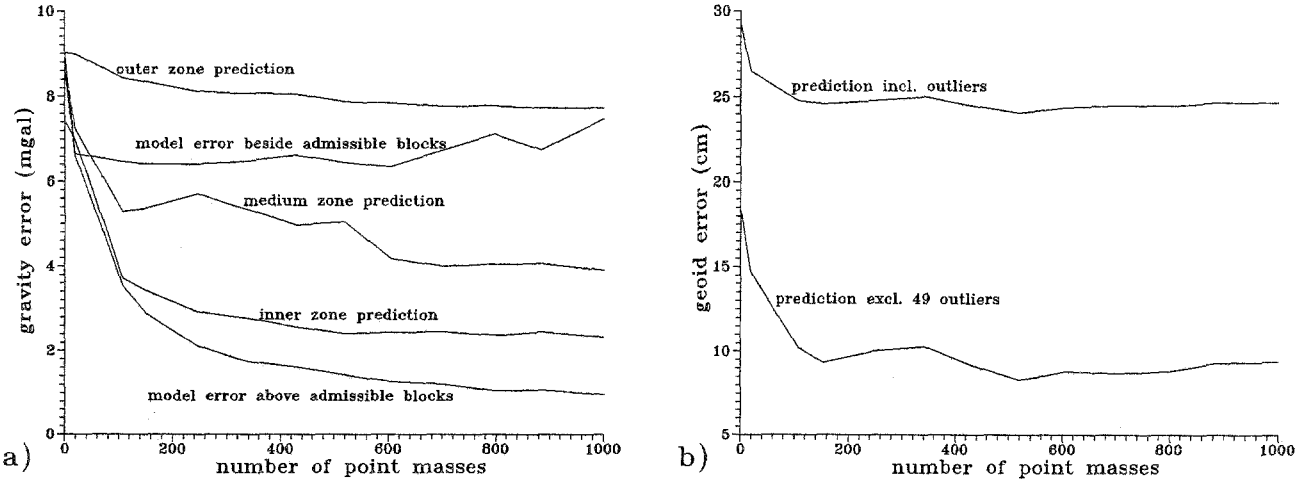

Figure 6: Errors (a:gravimetry, b:altimetry) versus number of point masses using gravimetric observations only. For the model error definition see section 2.1 and 2.3.

the admissible blocks, the point masses are hardly able to produce a good fit here.

In the following we focus on the comparison of the computed gravimetric geoid with altimetry data. For this purpose a bias and a tilt are subtracted from their differences in the Gulf area. This must be done because neither the SEASAT data (affected by orbital errors) nor the gravimetric data contain sufficient information on the datum of the geoid. Accordingly, only geoid height *differences* between points can be obtained precisely while the corresponding error increases with the distance of the points.

First of all, the SEASAT-data are likely to be gross error contaminated. Tscherning (1990) found 0.5–1.0% gross errors in two coastal regions of this area, he applied a detection strategy based on collocation. We use a simple 3σ-criterion instead: recursively, observation values with the maximum absolute residual (difference between observed value and model prediction) are deleted as long as more residuals exceed in absolute value three times the standard deviation than this would happen for Gaussian distribution (approx. 0.3%). This leads to 49 (=5.3%) suspected gross errors corresponding to the best solution including those errors (500 point masses, see Fig. 6b). However, taking other solutions has little effect on the outliers found. Probably, we have eliminated also some "good" observations, but we prefer to play it safe. By this we don't run the risk of distorting the subsequent combined solution.

Fig. 6b shows the accuracy estimate after discarding these gross errors. The geoid prediction appears to be best for 500 point masses again, here we achieve ± 8.3 cm. This is also the observation error for the SEASAT-data. Therefore, the computed geoid is supposed to be even more precise.

Fig. 7 shows the "sign pattern" of the residuals, they

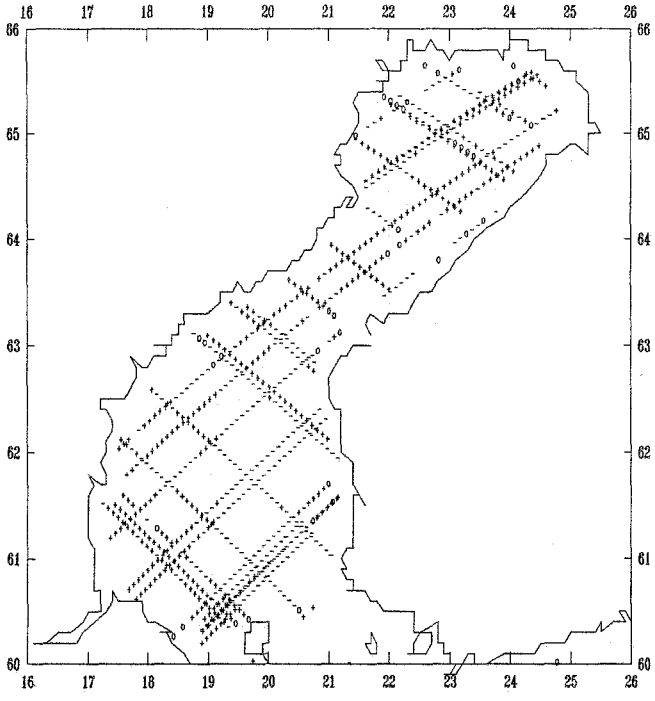

Figure 7: Distribution of the SEASAT-altimetry data. + and – indicate observed–predicted value for 500 point masses positive and negative, respectively. O means suspected outlier.

still contain a long wavelength part. [3] Vermeer (1984) did not find such features, he identified his differences as SEASAT noise. However, if we blame our point mass solution for this, we can hardly explain the precise fit. This effect is rather likely to be due to shortcomings in the crossover adjustment. Vermeer (priv. comm.) proposed to repeat the crossover adjustment after outlier elimination in order to avoid possible distortions. Fig. 7

[3] This corroborates doubts concerning the justification of the outlier detection strategy.

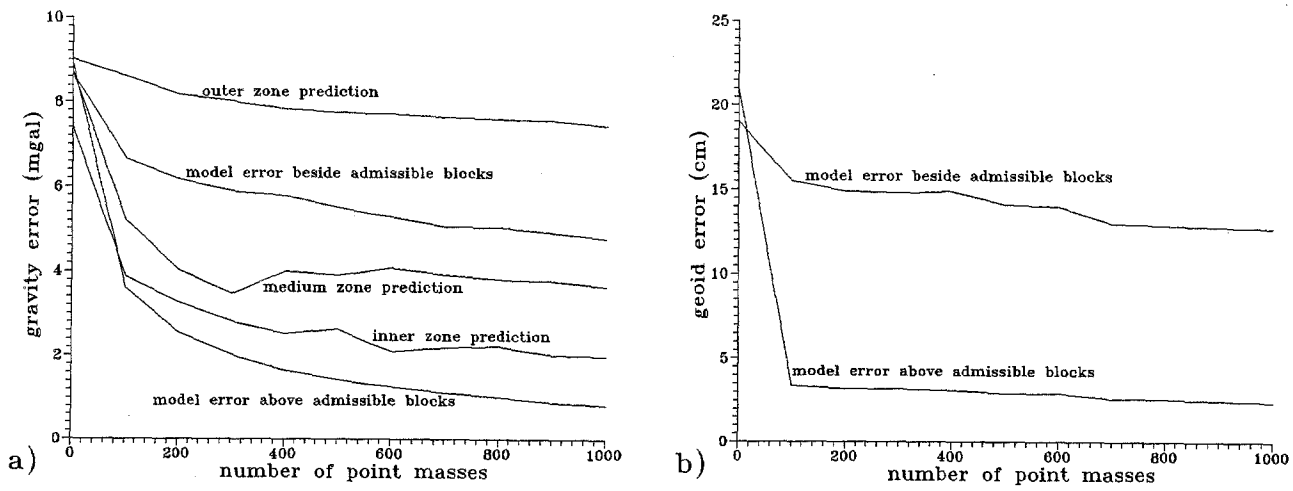

Figure 8: Errors (a:gravimetry, b:altimetry) versus number of point masses for the combined solution. For the model error definition see section 2.1 and 2.3.

also shows the detected outliers to accumulate along the coasts.

5 COMPUTATIONS COMBINING GRAVIMETRY AND ALTIMETRY DATA

We investigate the possibilities of using different kinds of data in the point mass optimization. The question is: Can the altimetry data really improve the solution? Doubts are well justified because the gravimetric solution has already reached the level of SEASAT-noise.

The computations are repeated using also the cross-over-adjusted SEASAT-data with latitudes larger than 57° as observations. Excluding the 49 detected outliers we find 1428 altimetry data. We redetermine the point mass limits with respect to these data, this yields 166 admissible blocks. The area above contains 73% of the altimetric and 84% of the gravimetric observations used.

As prediction quantities we use the 211 gravity anomalies in Fig. 3. They may decide whether improvement is achieved using altimetry or not. Fig. 8 shows the behaviour of certain error figures during increasing the number of determined point masses. For 1000 point masses we obtain ±2.0 mgal, ±3.6 mgal and ±7.4 mgal for the inner, medium and outer zone, respectively. This is clearly an improvement compared to the pure gravimetric solution. For the final geoid map see Fig. 9.

Of particular interest is the obtained spatial distribution of the computed point masses, it is also depicted in Fig. 9. The question, whether it has something to do with the density distribution of the Earth in this area, is beyond the scope of this paper. We believe that it is rather an image of the data densities and the data accuracies. There is still a lot of work to be done in this field.

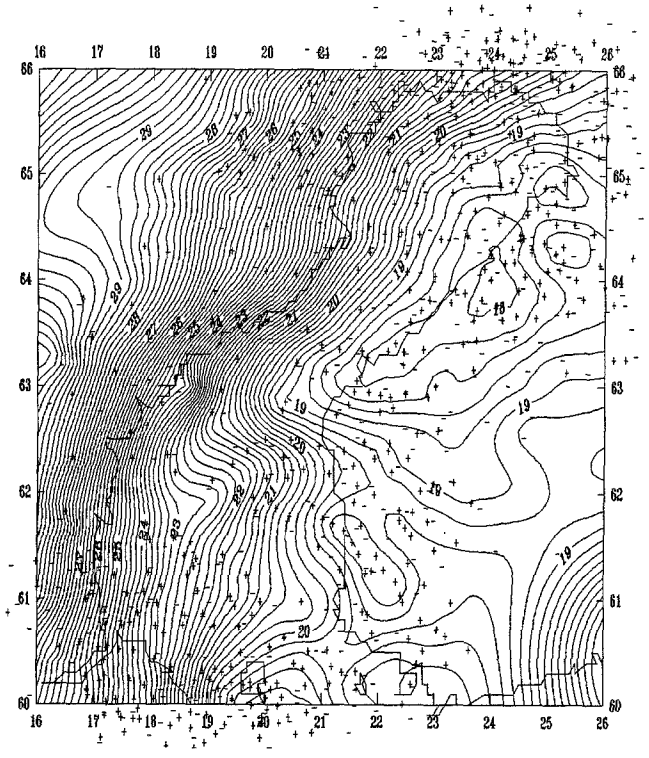

Figure 9: The geoid map (contour interval 0.20 m) and the distribution of the 1000 point masses obtained in the combined solution. + and − means positive and negative magnitude, respectively.

6 FURTHER REFINEMENTS

a) The approach of section 2.1 works fine, but does not fit completely in the general concept of variance-covariance estimation. Additionally, a maximum-likelihood estimate for σ_T was derived and investigated (Lehmann and Barthelmes 1992), the result suggests some changes of minor significance in the described procedure, here we state it only under the (practically fulfilled) con-

ditions

$$\mathbf{C}_d = \mathrm{diag}\{c_d^i\} \quad ; \quad \mathbf{C}_T = \mathrm{diag}\{c_T^i\}. \tag{9}$$

The estimate desired is the solution of

$$\sum_{i=1}^{N_d} \frac{\frac{(g^i(\mathbf{m}) - d_{obs}^i)^2}{c_d^i + \sigma_T^2 c_T^i} - 1}{\sigma_T^{-2} c_d^i / c_T^i + 1} = 2 \tag{10}$$

for σ_T, which again can be found iteratively.

b) One effect observed in this study was the accumulation of point masses at the upper depthlimits, the more the total number of point masses increases the more conspicuous it becomes. This is a somewhat unnatural behaviour, because those constraints are poorly defined and should not affect the model that drastically. Indeed, the concept of depthlimits for the point masses can be regarded as adding prior information, the corresponding probability distributions for the depth parameters are the uniform distributions over the intervals (D_{min}^i, D_{max}^i). As it is *invented* information, it should be as less informative as possible (maximum-entropy-principle). Strictly following this line of reasoning leads to a *Gamma-distribution* for the depth parameters. This clearly avoids the effect described above.

c) Nonlinear estimates are generally biased. Investigations based on the gravity anomalies in the Gulf of Bothnia showed the bias due to nonlinearity to be always less than half the noise (Lehmann 1992), thus it does not represent the largest share of the uncertainties in the results.

7 CONCLUSIONS

The method of free-positioned point masses extended in the described way turned out to be suitable and powerful also for ill-designed and complex problems in gravity field modelling. The results are remarkably good even in presence of data gaps and locally different data accuracies.

The gravity data in and near the Gulf of Bothnia allow the computation of a pure gravimetric geoid by means of this method. The best solutions differ from some highly precise gravity anomalies, excluded in advance, and the crossover-adjusted SEASAT-altimetry data in this region by about ±2.3 mgal and ±8.3 cm, respectively. However, the geoid is supposed to be even more precise than the altimetry comparison indicates.

Furthermore, the method has been proven to be able to use different types of data such as gravity anomalies combined with altimetry measurements. In fact, the predicted gravity anomalies fit better in the combined solution, here we obtain ±2.0 mgal.

In both solutions, the resulting geoid must be seen as a surface with only weak absolute orientation.

Both the reference model and the local model consist exclusively of free-positioned point masses. As already shown for the first their number is amazingly small for the second as well: We achieved remarkable accuracies for such a large number of observations (more than 11000) using only 500...1000 point masses. This gives a data compression factor of 3...5.

Comparisons with standard methods of geoid determination are not made. We believe, the advantage of this approach is the capability of incorporating very general geophysical knowledge via prior information for the model parameters.

Conclusions for the density distribution of the Earth are not drawn.

Acknowledgement

A large part of this work was done during a stay at the University of Copenhagen and the Danish National Survey and Cadastre. The author wishes to thank for the grant kindly provided by the Danish Research Academy. The author is indebted to Prof. C.C. Tscherning, M. Vermeer, R. Forsberg and P. Knudsen for their valuable advice and suggestions, and for providing the data sets as well as useful software tools (e.g. GRAVSOFT package). Special mention deserves M. Vermeer for his guidance in this work. Furthermore, thanks are due to F. Barthelmes and R. Dietrich for suggesting to undertake this study, for many fruitful discussions and for making available the point mass program of F. Barthelmes. The remarks of this journal's reviewers are also highly appreciated.

References

Anderson AJ, Scherneck HG (1981) The Geoid of the Baltic and the Gulf of Bothnia Obtained from SEASAT Altimetry Data. Dept. of Geod. Univ. of Uppsala, Rep. 10, Uppsala

Barthelmes F (1986) Untersuchungen zur Approximation des äußeren Gravitationsfeldes der Erde durch Punktmassen mit optimierten Positionen. Veröff. d. Zentr. Inst. f. Phys. d Erde, Nr. 92, Potsdam

Barthelmes F, Dietrich R (1990) Use of Point Masses on Optimized Positions for the Approximation of the Gravity Field. Proc. 1st Intern. Geoid Comm. Symp., Milan 11–13 June 1990

Barthelmes F, Dietrich R, Lehmann R (1991a) Global Gravity Field Modelling by Overlaying of Point Mass Models with Different Resolutions. Presented at the XVI General Assembly of the EGS, Wiesbaden 22–26 April 1991

Barthelmes F, Dietrich R, Lehmann R (1991b) Representation of the Global Gravity Field by Point Masses on Optimized Positions Based on Recent Spherical Harmonics Expansions. Presented at the XX General Assembly of the IUGG, Vienna 11–24 August 1991

Forsberg R (1984) A Study of Terrain Reductions, Density Anomalies and Geophysical Inversion Methods in

Gravity Field Modelling. Dept. of Geod. Sci., Rep. 355, Ohio State Univ., Columbus

Forsberg R (1990) A New High-Resolution Geoid of the Nordic Area. Proc. 1st Intern. Geoid Comm. Symp., Milan 11–13 June 1990

Forsberg R, Tscherning CC (1981) The Use of Height Data in Gravity Field Approximation by Collocation. J. Geophys. Res. 86:7843-7854

Heikinnen M (1981) Solving the shape of the earth by using digital density models. The Finnish Geod. Inst., Rep. 81:2, Helsinki

Lehmann R (1992) Nonlinear Gravity Field Inversion Using Point Masses – Diagnosing Nonlinearity. Proc. 7th Intern. Symp. "Geodesy and Physics of the Earth", Potsdam, 5–10 October 1992

Lehmann R, Barthelmes F (1992) Detection and Estimation of Model Errors in Geoid Computations by Gravimetric Inversion. Presented at the Workshop on Mathematical-geodetic methods for the determination of geoid and topography, Lambrecht 4–8 May 1992

Rapp RH, Pavlis NK, Wang YM (1991) High Resolution Gravity Models Combining Terrestrial and Satellite Data. Presented at the XX General Assembly of the IUGG, Vienna 11–24 August 1991

Tarantola A (1987) Inverse Problem Theory. Elsevier Amsterdam

Tscherning CC (1985) Geoid Modelling Using Collocation in Scandinavia and Greenland. Marine Geodesy 9:1-6

Tscherning CC (1990) A Strategy for Gross-Error Detection in Satellite Altimetry Data Applied in the Baltic Sea Area for Enhanced Geoid and Gravity Determination. Proc. 1st Intern. Geoid Comm. Symp., Milan 11–13 June 1990

Vermeer M (1982) The Use of Mass Point Models for Describing the Finnish Gravity Field. Proc. 9th meeting of the Nordic Geodetic Commission, Gävle, Sweden 13–17 Sept. 1982

Vermeer M (1983) A new SEASAT Altimetric Geoid for the Baltic. The Finnish Geod. Inst., Rep. 83:4, Helsinki

Vermeer M (1984) Geoid Studies on Finland and the Baltic. The Finnish Geod. Inst., Rep. 84:3, Helsinki